PHYSICAL REVIEW B VOLUME 60, NUMBER 16 15 OCTOBER 1999-II

Electronic structure of self-assembled InAs quantum dots in InP: An anisotropic quantum-dot system

H. Pettersson, R. J. Warburton, and J. P. Kotthaus
Center for Nanoscience and Sektion Physik, Ludwig-Maximilians-Universität, Geschwister-Scholl-Platz 1, D-80539 Munich, Germany

N. Carlsson, W. Seifert, M.-E. Pistol, and L. Samuelson
Division of Solid State Physics, Lund University, Box 118, S-221 00 Lund, Sweden

(Received 3 December 1998; revised manuscript received 9 March 1999)

The electronic structure of self-assembled InAs quantum dots embedded in an InP matrix has been investigated using Fourier-transform infrared spectroscopy and capacitance spectroscopy. We observe a splitting of about 25 meV between the conduction-band excited states. We argue that this is likely to be a consequence of a strong anisotropy in the lateral size of the dots. Furthermore, we observe a replica in the absorption spectrum, shifted by about 160 meV from the fundamental, which we attribute to an excited heavy-hole state. The InAs/InP dots can be well described in a simple adiabatic approach with a hard quantum well-like potential for the vertical confinement and a soft anisotropic harmonic potential for the lateral confinement.
[S0163-1829(99)50636-X]

During the last few years a lot of attention has been devoted to the growth and characterization of self-assembled quantum dots (SAD's). The strong interest in these systems is motivated by their potential for future high-speed electronic devices and by their intriguing atomiclike properties. Crucial issues are the shape and composition of the dots that determine the electronic structure. For buried dots the shape and composition are typically not known with any precision. The electronic structure has been addressed with spectroscopic methods, typically photoluminescence (PL) and photoluminescence excitation (PLE), and compared to the results of theoretical calculations that assume a particular shape. However, there are difficulties in interpreting the results of these spectroscopic studies, in particular PLE, which can be complicated by highly energy-dependent relaxation processes.[1,2] This means that it is generally difficult to compare the results to a particular model of the dots. A very promising experimental approach is to measure the absorption of light by the quantum dots as was recently demonstrated for InAs dots in GaAs.[3] This technique measures directly the energies and oscillator strengths of the interband transitions. We report here absorption measurements on InAs dots embedded in InP which, together with capacitance spectroscopy, give an accurate picture of the electronic structure.

Most experimental studies have concentrated on the optical properties of InAs dots in GaAs (for example, Refs. 1–3) and InP dots in $Ga_xIn_{1-x}P$.[4] An interesting quantum dot system, of which very little is known, is InAs dots embedded in InP. As for the other systems, homogeneous dots can be self-assembled using Stranski-Krastanov growth.[5] A strong luminescence of these dots at about 1.65 μm has been reported,[6] which makes them well suited for optoelectronic communication devices. Furthermore, the binding energy of holes is particularly large, about 400 meV,[7] which makes this material system also attractive for memory devices. In this paper, we report a detailed investigation of the electronic structure of these technologically interesting dots using a variety of techniques.

The samples used in this study were grown by metal-organic chemical-vapor deposition on semi-insulating substrates. Details on the growth of InAs dots in InP can be found in Ref. 6. The self-organized InAs dots are incorporated in a MISFET type of heterostructure.[8–11] The dots are buried beneath a 150-nm InP blocking barrier and separated from a highly doped back contact by a 25-nm InP tunneling barrier. From the geometry of the device, a change of voltage on the gate implies a seven times smaller change of electrostatic potential at the position of the dots. This factor 7 is referred to as the lever arm. The samples were processed with an Ohmic contact to the back electrode and a semitransparent gate electrode. From atomic force micrographs of samples with dots on the surface, we can expect that the buried dots are randomly distributed with a density of about 2×10^{10} cm^{-2}. The surface dots are typically 6 nm high and noticeably elongated along the [−110] direction. Average base dimensions are about 35 nm (hereafter referred to as L_x) along [110] and 45 nm (L_y) along [−110].[6]

Figure 1 summarizes the capacitance spectroscopy (CS) measurements. Measuring the differential capacitance between the top Schottky electrode and the buried back electrode while sweeping the dc bias from 0.5 to −2.0 V reveals three resonances that correspond to electron tunneling from the back electrode through the 25-nm InP barrier into discrete states in the conduction band of the InAs dots (see inset). The strong increase in capacitance at about 0.4 V is due to electron tunneling into the InAs wetting layer. The area under each resonance gives the amount of charge that has tunneled into the dots. Since the concentration of quantum dots is known from atomic force micrographs of samples grown under identical conditions, we can relate the area under the peaks to the average number of electrons loaded into each dot. As shown in Fig. 1, we subtract the background signal and fit the resonances to three Gaussian functions. We find that each Gaussian has the same area and that this area corresponds to loading the dots with two additional electrons, i.e., there is a ground state and two excited

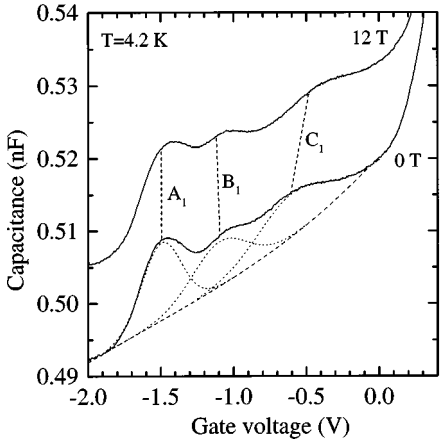

FIG. 1. Capacitance against gate voltage for 0 and 12 T measured at 4.2 K. The observed resonances correspond to charging of the electron levels in the dots. The data at 0 T were fitted to a background signal (dashed line) and to three Gaussians (dotted lines). The dashed lines between the 0 and 12 T traces connect the maxima of the fitted Gaussians showing how the splitting between the second and third charging peaks increases with magnetic field. The inset shows the conduction-band profile of the device in the growth direction with the Fermi levels in the gate contact, E_{FS}, and back contact, E_{FB}.

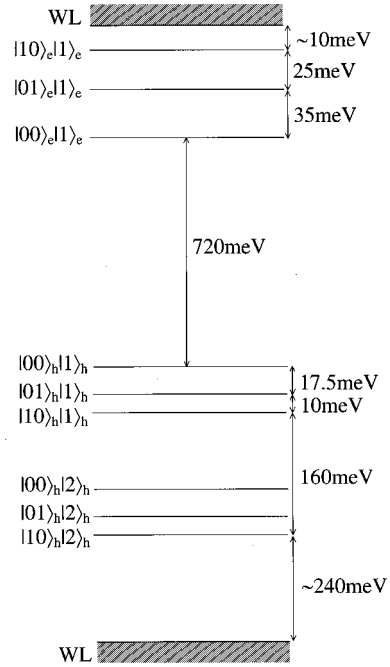

FIG. 2. An energy level diagram of the electronic structure of InAs dots in an InP matrix as determined from the CS and FTIR experiments.

states all with degeneracy 2. The excited state has degeneracy 4 in a rotationally symmetric system. We find, however, that this degeneracy is lifted here.

In order to classify the wave functions further, we assume that we can separate the vertical confinement and the lateral confinement. Such an adiabatic approach is justified by the large disparity in the vertical and lateral dimensions of the dots. In the vertical direction (z) we have a quantum well-like potential; in the lateral plane (x,y) it is reasonable to assume that the confinement potential is close to parabolic, with eigenstates $|n_x n_y\rangle$ with eigenenergies $E_{x,y}=\hbar\omega_x^e(n_x+1/2)+\hbar\omega_y^e(n_y+1/2)$. The entire wave function is then $|n_x n_y\rangle|n_z\rangle$. In Ref. 7 a complicated eight-band $k\cdot p$ model for calculating the ground-state binding energies of electrons and holes in InAs/InP dots was used. However, the exact shape and size of the buried dots still has to be clarified and so we have chosen here a simpler model that we show to be a good approximation. It should be emphasized, however, that the energy level diagram we present in Fig. 2 is not dependent on the details of our model but represents the energetic positions of the levels as determined from our experiments.

The three resonances in the CS correspond to tunneling into the $|00\rangle_e|1\rangle_e$ (peak A_1), the $|01\rangle_e|1\rangle_e$ (peak B_1), and the $|10\rangle_e|1\rangle_e$ (peak C_1) states. The positions of the peaks A_1, B_1, and C_1 do not give the single-particle splittings $\hbar\omega_x^e$ and $\hbar\omega_y^e$ directly as they are influenced by the Coulomb charging energies. The charging energies can be measured directly if the individual peaks for successive tunneling into the same state (Coulomb blockade) can be observed. We do not resolve this splitting as the inhomogeneous broadening is slightly too large. The capacitance peaks have full widths of at least 60 meV yet typical charging energies in self-assembled quantum dots are 20–30 meV.[10–12] In order to extract the single-particle splittings from the data in Fig. 1, we calculate the Coulomb energies for a particular ground-state configuration using perturbation theory, as in Ref. 13 but with an asymmetric lateral potential. For instance, the Coulomb interaction between two electrons in the ground state is given by

$$\Delta E_{00}=\frac{e^2}{4\pi\epsilon_0\epsilon_r}\frac{1}{2\sqrt{2\pi}}\int_0^{2\pi}\frac{d\theta}{\sqrt{l_x^2\cos^2\theta+l_y^2\sin^2\theta}},$$

an elliptic integral. $l_{x,y}^e=\sqrt{\hbar/m_e^*\omega_{x,y}}$ are the effective lengths associated with the quantization energies $\hbar\omega_x^e$ and $\hbar\omega_y^e$. We find that the interactions between electrons in different states can all be expressed in terms of elliptic integrals. The gate voltage is converted into an energy with the lever arm.[8–12] The Coulomb blockade conditions are then given by the voltages at which the N and $N+1$ electron ground states are degenerate. Peaks A_1, B_1, and C_1 each correspond to the average of two Coulomb blockade peaks. We take the InP effective mass (0.075) because the GaAs mass and not the InAs mass has been found to be appropriate for InAs dots in GaAs.[11] Applying this model to the data in Fig. 1 allows us to estimate the two quantization energies, $\hbar\omega_x^e$ and $\hbar\omega_y^e$, from the CS to be 60 ± 5 and 35 ± 5 meV, respectively.

We can support these values with a number of observations. First, we have performed preliminary far infrared spectroscopy on these dots where we indeed see a weak resonance at 57 meV as shown in Fig. 3. This peak is consistent with a transition between $|00\rangle_e|1\rangle_e$ and $|10\rangle_e|1\rangle_e$. The other peak at 46 meV in Fig. 3 has a very weak dependence on the magnetic field and lies extremely close to the Reststrahlen band and so it probably corresponds to a phonon-related interaction. A strong interface phonon has been observed in far infrared spectroscopy on charge-tunable InAs/GaAs dots.[11]

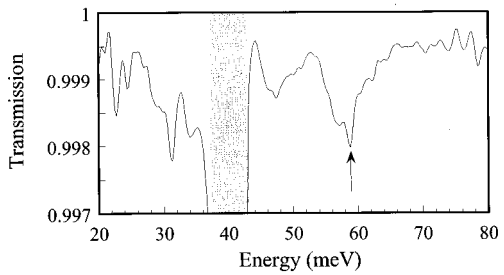

FIG. 3. Far infrared spectrum taken at gate voltage 0 V and at 4.2 K. A reference spectrum was taken at -2 V. The transmission of the sample was too small for useful data in the range 37–43 meV.

The transition between $|00\rangle_e|1\rangle_e$ and $|01\rangle_e|1\rangle_e$ could not be observed, probably because it coincides energetically with the Reststrahlen band. Second, our interpretation that the peaks B_1 and C_1 in the CS correspond to tunneling into the $|01\rangle_e|1\rangle_e$ and $|10\rangle_e|1\rangle_e$ states, respectively, is confirmed by the data in a magnetic field of 12 T (Fig. 1). The B_1 peak shifts to lower voltages and the C_1 peak shifts to higher voltages, which is exactly the behavior expected for the $|01\rangle_e|1\rangle_e$ and $|10\rangle_e|1\rangle_e$ states.[12–15] We note that our inferred $\hbar\omega_x^e = 60$ meV and $\hbar\omega_y^e = 35$ meV imply that the $|10\rangle_e|1\rangle_e$ state is almost degenerate with the $|02\rangle_e|1\rangle_e$ state. We find no evidence, however, for the existence of the $|02\rangle_e|1\rangle_e$ state both in CS and Fourier-transform infrared spectroscopy (FTIR) implying that this state lies too close to the wetting layer continuum for us to observe it. We use this to position the conduction-band wetting layer in the level diagram of Fig. 2. The implication is that $\hbar\omega_y^e$ must be larger than 30 meV. Finally, we can estimate the charging energy for adding a second electron to the ground state, $|00\rangle_e|1\rangle_e$. At low excitation density we measure a PL linewidth of 50 meV. This is predominantly determined by fluctuations in the vertical direction and as these scale with the inverse of the effective mass, we can estimate that the broadening in the conduction band is approximately 40 meV. We then fit two Gaussians, each with a 40 meV width but with different peak energies, to curve A_1 to estimate a Coulomb energy of 20 meV. This is in rough agreement with the calculation above which gives 30 meV for this interaction.

We note that our measured $\hbar\omega_x^e$ and $\hbar\omega_y^e$ imply that $l_y^e/l_x^e = 1.3$, the same to within error as the anisotropy L_y/L_x determined from AFM. This suggests that the disparity in $\hbar\omega_x^e$ and $\hbar\omega_y^e$ arises from the anisotropy in the dots' size. An alternative explanation would be that the splitting arises from the strain field as calculations have shown that a splitting arises for highly facetted dots.[16] However, in this case the interband transitions should possess a polarization which is not the case for the present samples: any in-plane polarization is smaller than 10%. It is therefore likely that the splitting in the *p*-like states is related to the anisotropy in the dots' size.

The absorption FTIR measurements were performed with a Fourier-transform spectrometer and InAs *p-i-n* diode as detector. Since the absorption of the quantum dots is only of the order of 10^{-5} to 10^{-4} a very stable and sensitive experimental setup is required.[3] We inserted a Si filter into the beam so that there is no above-barrier excitation of the

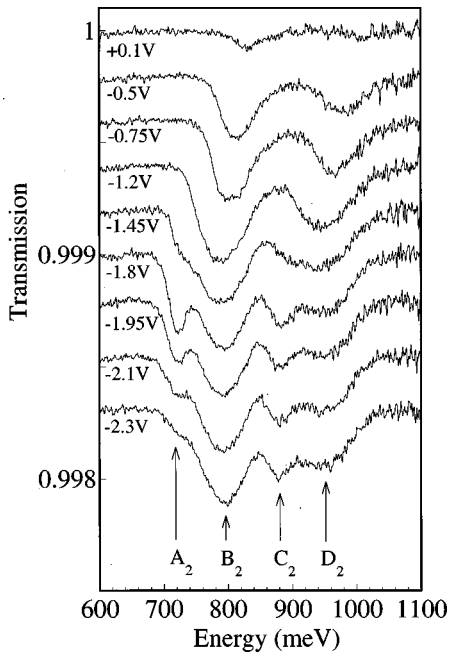

FIG. 4. Interband transmission spectra of the dots taken at different gate voltages and at 4.2 K. The traces are offset from 1 for clarity. In each case a reference spectrum was taken at 0.5 V.

sample. Figure 4 shows the spectral distribution of the transmission through the sample, recorded at different gate voltages, using in each case a trace at large and positive voltage as a reference spectrum. At a gate voltage of -2.3 V three strong resonances, B_2, C_2, and D_2 are observed. An additional weak peak at 720 meV is also observed which corresponds well to the low energy peak we observe in PL and we therefore attribute it to the ground-state exciton (peak A_2). Interestingly, decreasing the bias to -1.8 V gradually increases the strength of the ground-state exciton absorption. We believe that the broadband excitation from the spectrometer creates a steady-state occupancy of holes in the ground state of the dots, $|00\rangle_h|1\rangle_h$, blocking the interband absorption. The light creates electron-hole pairs in the dots whereafter the electrons escape, owing to a very small tunneling time, leaving behind the holes.[7,17] From the capacitance trace in Fig. 1, it is evident that at a voltage of -1.8 V electrons start to tunnel into the electron ground state. They are then free to recombine with the excess holes. This neutralization of the charge in the dots increases the strength of the ground-state exciton absorption. At higher voltages still, the ground state is occupied by electrons, which also block the interband absorption. Consequently, the ground-state absorption can never acquire its full oscillator strength.

A further decrease in gate bias results in a simultaneous decrease in the height of peaks A_2 and C_2 and at about -1.2 V both peaks have disappeared completely. At this voltage the CS of Fig. 1 tells us that we have fully populated the ground state, $|00\rangle_e|1\rangle_e$. The implication is that A_2 and C_2 have the same final state which must be $|00\rangle_e|1\rangle_e$. The peaks disappear in the FTIR simply through Pauli blocking. The energy separation between peaks A_2 and C_2 amounts to some 160 meV and must arise from a splitting between the two initial states. We argue that such a large energy splitting for valence-band states must have its origin in two different

eigenstates for the strong vertical confinement of the dots. There are three possibilities for the higher hole state, $HH2$, $HH3$, or $LH1$. It might be thought that $HH2$-$E1$ is parity forbidden as for a quantum well. However, this selection rule may be strongly relaxed in the present case as there is no guarantee that the vertical confinement potential is inversion symmetric. $HH3$-$E1$ is in any case allowed, yet we estimate that the energy would be far too large. The $LH1$-$E1$ transition is also not forbidden by parity, but it should be pushed to much higher energy by the uniaxial strain. Also, the nature of the Bloch functions implies that the $LH1$-$E1$ transition is a factor of 3 weaker than the $HH1$-$E1$ transition, which is clearly not the case in Fig. 4. We therefore identify the excited hole level $|00\rangle_h|2\rangle_h$ as $HH2$. For comparison, we have calculated the energy splitting between the heavy-hole ground state and the first excited heavy-hole state for an InAs quantum well, with varying thickness, embedded in InP in the envelope function approximation. In this calculation we used a valence-band offset of 400 meV.[7] For a thickness of 4 nm we find an energy separation of about 150 meV. A thickness of about 4 nm is a reasonable average height if we approximate our dots with elliptic-shaped disks, supporting our assignment.

When the bias is reduced even further, peaks B_2 and D_2 disappear simultaneously, again implying identical final states in the conduction band. The full widths at half maximum (FWHM's) of both peaks are significantly larger than those of A_2 and C_2 and this would suggest that both B_2 and D_2 are made up of two unresolved transitions. Our interpretation is that B_2 contains $|01\rangle_h|1\rangle_h$ to $|01\rangle_e|1\rangle_e$ and $|10\rangle_h|1\rangle_h$ to $|10\rangle_e|1\rangle_e$, and D_2 $|01\rangle_h|2\rangle_h$ to $|01\rangle_e|1\rangle_e$ and $|10\rangle_h|2\rangle_h$ to $|10\rangle_e|1\rangle_e$. Here $|10\rangle_h$ and $|01\rangle_h$ are the anisotropic harmonic oscillator eigenstates for holes with transition energies $\hbar\omega_x^h$ and $\hbar\omega_y^h$. The integrated absorption of B_2 supports this view. Theoretically, we can expect an integrated absorption of 2.1×10^{-5} eV per transition.[3] B_2 has an absorption of 4×10^{-5} eV implying two transitions.

The energy separation between peaks A_2 and B_2 amounts to about 70 meV which corresponds to $\hbar(\omega_x^e+\omega_y^e)/2+\hbar(\omega_x^h+\omega_y^h)/2$. Since $\omega_x^e/\omega_y^e\approx\omega_x^h/\omega_y^h$ we estimate that $\hbar\omega_x^h=27.5$ meV and $\hbar\omega_y^h=17.5$ meV. Likewise, the separation between the peaks C_2 and D_2 is also about 70 meV. Fitting two Gaussian functions with FWHM=50 meV to peak B_2 we deduce a splitting of about 38 ± 5 meV that is in excellent agreement with the expected $\hbar(\omega_x^e-\omega_y^e)+\hbar(\omega_x^h-\omega_y^h)$.

All this information is summarized in Fig. 2 which shows the electronic structure of self-assembled InAs dots in InP obtained from the combined analysis of the optical and electrical data. The position of the wetting layer in the valence band was determined from its photoluminescence energy. Electron and hole confinement energies have also been measured in this system by DLTS.[7] However, this technique measures escape rates of carriers out of the dots into the InP barrier material and not into the InAs wetting layer. Excitation must occur into states that are a few units of thermal energy away from the InP barrier. In contrast, we estimate here the barrier heights between the dot levels and the onset of the InAs continuum. The consequence is that the barrier heights determined by DLTS are higher than the barrier heights we estimate here.

In conclusion, we emphasize the two key results of our experiments on InAs/InP quantum dots. First, there is a splitting between the *p*-like states in the conduction band. Second, there are states high up in the valence band that have the same lateral character as states close to the valence-band edge. We argue that the splitting of the *p*-like states arises most likely as a consequence of the dots' elongation along $[-110]$. The valence-band states are strongly suggestive of an adiabatic character, and are certainly related to the deep valence band found in this system.

The authors gratefully acknowledge fruitful discussions with A. O. Govorov, R. J. Luykens, and A. Lorke. One of the authors (H.P.) would also like to thank the European Community for financial support and the group at LMU for its hospitality. This work was supported also by the Deutsche Forschungsgemeinschaft via SFB 348.

[1] R. Heitz *et al.*, Appl. Phys. Lett. **68**, 361 (1996).
[2] K. H. Schmidt *et al.*, Phys. Rev. B **54**, 11 346 (1996).
[3] R. J. Warburton *et al.*, Phys. Rev. Lett. **79**, 5282 (1997).
[4] D. Hessman *et al.*, Appl. Phys. Lett. **69**, 749 (1996).
[5] W. Seifert *et al.*, Prog. Cryst. Growth Charact. Mater. **33**, 423 (1996).
[6] N. Carlsson *et al.*, J. Cryst. Growth **191**, 347 (1998).
[7] H. Pettersson *et al.* (unpublished).
[8] R. C. Ashoori *et al.*, Phys. Rev. Lett. **71**, 613 (1993).
[9] H. Drexler *et al.*, Phys. Rev. Lett. **73**, 2252 (1994).
[10] G. Medeiros-Ribeiro *et al.*, Phys. Rev. B **55**, 1568 (1997).
[11] M. Fricke *et al.*, Europhys. Lett. **36**, 197 (1996).
[12] B. T. Miller *et al.*, Phys. Rev. B **56**, 6764 (1997).
[13] R. J. Warburton *et al.*, Phys. Rev. B **58**, 16 221 (1998).
[14] Q. P. Li *et al.*, Phys. Rev. B **43**, 5151 (1991).
[15] F. M. Peeters, Phys. Rev. B **42**, 1486 (1990).
[16] C. Pryor *et al.*, Phys. Rev. B **56**, 10 404 (1997).
[17] M. C. Bödefeld *et al.*, Appl. Phys. Lett. **74**, 1839 (1999).